



Published in final edited form as:

ACS Catal. 2018 January 5; 8(1): 59–62. doi:10.1021/acscatal.7b03323.

Copper-Containing Catalytic Amyloids Promote Phosphoester Hydrolysis and Tandem Reactions

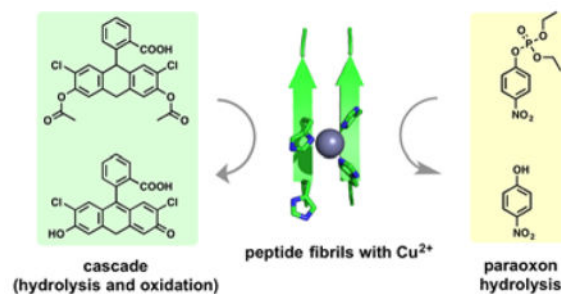
Zsófia Lengyel, Caroline M. Rufo, Yurii S. Moroz[†], Olga V. Makhlynets, and Ivan V. Korendovych*

Department of Chemistry, Syracuse University, 111 College Place, Syracuse, NY 13244

Abstract

Self-assembly of short *de novo* designed peptides gives rise to catalytic amyloids capable of facilitating multiple chemical transformations. We show that catalytic amyloids can efficiently hydrolyze paraoxon, a widely used, highly toxic organophosphate pesticide. Moreover, these robust and inexpensive metal-containing materials can be easily deposited on various surfaces producing catalytic flow devices. Finally, functional promiscuity of catalytic amyloids promotes tandem hydrolysis/oxidation reactions. High efficiency discovered in a very small library of peptides suggests an enormous potential for further improvement of catalytic properties both in terms of catalytic efficiency and substrate scope.

Graphical Abstract



Keywords

cascade reaction; self-assembly; peptides; copper; paraoxon

Self-assembly of short peptides presents a facile method of producing a large number of extremely functionally and structurally diverse amyloid-like assemblies.^{1–11} Recently we have shown that self-assembly of *de novo* designed peptides in the presence of metal ions

Corresponding Author: ikorendo@syr.edu.

[†]Present Addresses

Department of Chemistry, Taras Shevchenko National University of Kyiv, 64 Volodymyrska St., Kyiv 01601, Ukraine.

Author Contributions

The manuscript was written through contributions of all authors. All authors have given approval to the final version of the manuscript.

Supporting Information. Details of peptide synthesis, characterization, and kinetic studies. The Supporting Information is available free of charge on the ACS Publications website.

produces catalytic amyloids capable of efficient catalysts of a number of hydrolytic and redox chemical transformations.^{12–14} The catalytic efficiency of these nanoassemblies in model reactions is higher than that of some enzymes by weight and can be further improved by synergistic interactions observed in mixtures of peptides with different sequences. The resulting fibrils are extremely homogeneous, can function under high pressure,¹⁵ and exhibit moderate substrate preference.¹⁶ Moreover, catalytic metalloamyloids with diverse sets of primary sequences^{17–19} and metal ions²⁰ have been reported.

Given the exciting possibilities in catalysis provided by amyloid assemblies we aimed to embark beyond simple model substrates and determine whether catalytic amyloids can be successfully employed to hydrolyze paraoxon, a widely used, highly toxic organophosphate pesticide (Scheme 1), that contributes to estimated three million organophosphate poisonings a year worldwide.²¹ Moreover, chemical similarity of paraoxon to toxic nerve agents, makes it a useful test system to develop efficient and practical strategies for chemical weapons remediation. Paraoxon is a challenging substrate for hydrolysis (background hydrolysis $k_{\text{uncat}} = 7.97 \times 10^{-7} \text{ min}^{-1}$ at pH 7.8),²² thus this pesticide persists in the environment for a prolonged period of time. While a number of highly efficient paraoxonases have been already developed using directed evolution of related proteins,²³ catalytic amyloids offer a number of practical advantages such as robustness, low cost and ease of modification.

Hydrolysis of paraoxon is often facilitated by metalloco-factors, Cu^{II} being one of the most reactive ones.²⁴ Given the established ability of catalytic amyloids to bind this metal ion^{13–14} we have tested the ability of several previously synthesized peptides to catalyze paraoxon hydrolysis in the presence of copper.

The results of the screening (Fig. S1, Supporting Information) show that catalytic amyloids can provide substantial acceleration of paraoxon hydrolysis over the background rate. Peptide **7IY** (Ac-IHIHIYI-NH₂) showed very high activity in the initial screen, thus we chose it for in depth characterization. Interestingly, several peptides with very minor differences in primary sequences as compared to **7IY** showed activity that is somewhat lower than that of free copper ions, consistent with unproductive binding of the metal ion to peptide.

7IY forms amyloid-like fibrils in the presence of copper as evidenced by atomic force microscopy (AFM), circular dichroism (CD) and thioflavin T (ThT) fluorescence data (Fig. 1a–b, Fig. S2, Supporting Information). Interestingly ThT fluorescence in the presence of copper fibrils is much diminished when compared to fibrils that do not contain the metal. This is consistent with fluorescence quenching by paramagnetic copper ions. The fibrils show well-defined block morphology, with most probable thickness of $\sim 2.5 \text{ \AA}$ consistent with a single bilayer of cross-beta oriented peptides (Fig. S3, Supporting Information) in agreement with previous SAXS¹⁸ and ssNMR²⁵ studies.

Formation of the fibrils is quite rapid – incubation of the peptides for 24 hours does not result in significant additional fibrillization (Fig. S2, Supporting Information). The dependence of the initial rate of hydrolysis as a function of substrate concentration (Fig. 1c)

can be fit to the Michaelis-Menten equation to yield kinetic parameters of $k_{\text{cat}} = 4.8 \pm 0.9 \times 10^{-3} \text{ min}^{-1}$, $K_{\text{M}} = 2.9 \pm 0.8 \text{ mM}$ and $k_{\text{cat}}/K_{\text{M}} = 1.7 \pm 0.6 \text{ M}^{-1}\text{min}^{-1}$. The pH profile of the activity (Fig. S4, Supporting Information) is consistent with a single water deprotonation step with an effective pK_{a} of 8.3. While the resulting $k_{\text{cat}}/k_{\text{uncat}}$ ratio of 3.5×10^3 at pH 8.0 is inferior to those observed for engineered enzymes,^{23, 26–28} it is on par with catalytic antibodies^{22, 29} and small molecule catalysts.^{30–32} It compares well to many polymer-based heterogeneous catalysts albeit it is difficult to draw direct comparison as experimental conditions vary widely (Table S1, Supporting Information).

7IY reaches its maximum activity at *ca.* 1 equiv of copper (Fig. S5, Supporting Information). EPR spectrum of Cu^{II} -bound **7IY** shows a typical Type II copper similar to the one observed in other catalytic amyloid peptides (Fig. S6, Supporting Information). The g_{\parallel} , g_{\perp} , and A_{\parallel} parameters are very similar to the ones observed for **7IQ** suggesting nearly identical metal coordination sphere.¹³ The lack of a charge transfer band corresponding to copper-phenolate interaction suggests that Tyr6 is not directly involved in copper coordination.

The comparison of the rates of paraoxon hydrolysis with those of the *p*-nitrophenylacetate (*p*NPA) is instructive. Consistent with the previous study¹⁸ **7IY** shows very high efficiency in hydrolyzing *p*NPA in the presence of zinc ($k_{\text{cat}}/K_{\text{M}} = 5888 \pm 195 \text{ M}^{-1}\text{min}^{-1}$). However, the rate of **7IY**-promoted *p*NPA hydrolysis in the presence of copper, while still quite significant, is much slower ($k_{\text{cat}}/K_{\text{M}} = 806 \pm 100 \text{ M}^{-1}\text{min}^{-1}$). The reverse trend is true for phosphoesters as copper-containing fibrils are more efficient in paraoxon hydrolysis (Fig. S7, Supporting Information).

Catalytic amyloids being heterogeneous catalysts provide a very significant degree of molecular control akin to that found in homogeneous catalysts. In order to explore practicality of use of catalytic amyloids we have created a flow catalyst. Catalytic amyloids prepared by addition of copper ions to **7IY** were filtered through a $0.22 \mu\text{m}$ polyethersulfone (PES) filter (Fig. 2). Once amyloids are formed and filtered through the PES support, very little peptide was observed in the filtrate (Fig. S8, Supporting Information). The resulting filter can be immediately used as a heterogeneous catalyst for hydrolysis of paraoxon in a flow system (Fig. 2). While the overall activity of the amyloids deposited on the filter is somewhat diminished as compared to the original suspension, multiple passes of the substrate solution can be done to facilitate paraoxon hydrolysis in a continuous manner. The simplicity of the catalyst deposition onto unfunctionalized filter support will greatly aid in practical applications that require easy catalyst separation and recycling.

Encouraged by high chemical versatility of catalytic amyloids we set out to explore whether they can simultaneously promote multiple reactions at the same time. High hydrolytic activity of copper-containing catalytic amyloids together with their ability to activate oxygen¹³ prompted us to explore whether they can facilitate cascade reactions that include hydrolytic and redox components. Cascade (also referred to as tandem) reactions are multi-step sequential chemical transformations that require formation of the first product for the initiation of the next step.³³ As a test substrate for cascade reactions we have chosen a well-established substrate - 2',7'-dichlorofluorescein diacetate (DCFH-DA) that normally

undergoes hydrolysis to produce 2',7'-dichlorofluorescin (DCFH), which in turn gets oxidized to yield highly fluorescent 2',7'-dichlorofluorescein (DCF), Scheme 1.³⁴ Alternatively, DCFH-DA can get first oxidized to DCF-DA followed by hydrolysis to produce DCF, although the overall rate of this path is slower.³⁵ The formation of product can be followed by fluorescence and/or appearance of the absorption band at 504 nm (Fig. S9, Supporting Information). The heterogeneous nature of copper-containing amyloids is expected to provide an additional kinetic advantage – the product of hydrolysis can associate with the catalytic amyloids for some degree (as evidenced by relatively low K_M values observed for a variety of substrates), thus creating a higher effective concentration for the oxidation step giving an overall boost in the observed kinetics.

We have tested ability of **7IY** to catalyze hydrolysis and oxidation of DCFH-DA. The results of kinetic experiments are shown in Table 1 and Fig. S10, Supporting Information. **7IY** *simultaneously* catalyzes hydrolysis *and* oxidation of DCFH-DA in buffer at pH 8.0 with the effective second order rate constants of $61 \pm 9 \text{ M}^{-1} \text{ min}^{-1}$; the background rate of the reaction under these conditions is essentially negligible (Table S2, Supporting Information). In order to gain mechanistic insight into this transformation we have measured the rate of oxidation of DCFH as well as the rate of hydrolysis of DCF-DA, a substitute for DCFH-DA as hydrolysis of DCFH-DA does not produce a convenient fluoro- or chromophore (Scheme 1).

The rate of the hydrolysis step is about 10-fold slower than the rate of oxidation in both cases, making it rate limiting. Interestingly, the rate of DCF-DA hydrolysis is about 2-fold lower than the overall rate of DCHF-DA conversion to DCF, meaning that the combined reaction rate is faster than the rate-limiting step.

This can be explained by either contribution of the alternative path (oxidation followed by hydrolysis) to the increase of overall rate or by a difference in the hydrolysis rate of DCF-DA compared to that of DCFH-DA. In order to test these hypotheses we tested the reactivity of a closely related peptide **7IQ** (Ac-IHIHIQI-NH₂), that has previously shown superior activity in redox catalysis,¹³ in DCFH-DA hydrolysis and oxidation. Despite very similar activities of **7IQ** and **7IY** in DCF-DA hydrolysis and DCFH oxidation, the overall conversion of DCFH-DA to DCF is almost 2-fold higher for **7IQ** ($97 \pm 7 \text{ M}^{-1} \text{ min}^{-1}$) than that of **7IY**. This observation essentially eliminates the possibility that DCF-DA is a poor substitute for DCFH-DA for kinetic studies and is consistent with multiple pathways for oxidation and hydrolysis simultaneously available for catalytic amyloids that result in the overall rate acceleration.

In summary, we have shown that catalytic amyloids are capable of facilitating hydrolysis of paraoxon, a challenging substrate of practical importance, by more than three orders of magnitude ($k_{\text{cat}}/k_{\text{uncat}}$). We have also demonstrated that catalytic amyloids can be easily utilized in flow cells. We have shown for the first time that promiscuity of catalytic amyloids allows them to facilitate tandem transformations. High activity of catalytic amyloids seen in a very limited library of short peptides suggests an incredible potential for further improvement of catalytic properties both in terms of catalytic efficiency and substrate scope.

Supplementary Material

Refer to Web version on PubMed Central for supplementary material.

Acknowledgments

Funding Sources

No competing financial interests have been declared. This work was supported by the NIH (grant GM119634 to I.V.K.), the NSF (grant 1332349 to I.V.K.) and the Alexander von Humboldt Foundation. The EPR facilities at Cornell (ACERT) are supported by an NIH grant P41GM103521.

AFM images were collected at the Argonne National Lab (Center for Nanoscale Materials). We thank Dr. Boris Dzikovski for assistance with EPR experiments.

References

1. Duncan KL, Ulijn RV. *Biocatalysis*. 2015; 1:67–81.
2. Maeda Y, Makhlynets OV, Matsui H, Korendovych IV. *Annu Rev Biomed Eng*. 2016; 18:311–328. [PubMed: 27022702]
3. Branco MC, Sigano DM, Schneider JP. *Curr Opin Chem Biol*. 2011; 15:427–434. [PubMed: 21507707]
4. Omosun TO, Hsieh MC, Childers WS, Das D, Mehta AK, Anthony NR, Pan T, Grover MA, Berland KM, Lynn DG. *Nat Chem*. 2017; 9:805–809. [PubMed: 28754939]
5. Swanekamp RJ, Welch JJ, Nilsson BL. *Chem Commun*. 2014; 50:10133–10136.
6. Liyanage W, Brennessel WW, Nilsson BL. *Langmuir*. 2015; 31:9933–9942. [PubMed: 26305488]
7. Fry HC, Garcia JM, Medina MJ, Ricoy UM, Gosztola DJ, Nikiforov MP, Palmer LC, Stupp SI. *J Am Chem Soc*. 2012; 134:14646–14649. [PubMed: 22916716]
8. Solomon LA, Kronenberg JB, Fry HC. *J Am Chem Soc*. 2017; 139:8497–8507. [PubMed: 28505436]
9. Burton AJ, Thomson AR, Dawson WM, Brady RL, Woolfson DN. *Nat Chem*. 2016; 8:837–844. [PubMed: 27554410]
10. Singh N, Kumar M, Miravet JF, Ulijn RV, Escuder B. *Chem – Eur J*. 2017; 23:981–993. [PubMed: 27530095]
11. Rubinov B, Wagner N, Rapaport H, Ashkenasy G. *Angew Chem Int Ed*. 2009; 48:6683–6686.
12. Rufo CM, Moroz YS, Moroz OV, Stöhr J, Smith TA, Hu X, DeGrado WF, Korendovych IV. *Nat Chem*. 2014; 6:303–309. [PubMed: 24651196]
13. Makhlynets OV, Gosavi PM, Korendovych IV. *Angew Chem Int Ed*. 2016; 55:9017–9020.
14. Sternisha A, Makhlynets O. *Synthetic Protein Switches: Methods and Protocols*. Stein V, editorSpringer New York; New York: 2017. 59–68.
15. Luong TQ, Erwin N, Neumann M, Schmidt A, Loos C, Schmidt V, Fändrich M, Winter R. *Angew Chem Int Ed*. 2016; 55:12412–12416.
16. Heier JL, Mikolajczak DJ, Böttcher C, Koksche B. *Pept Sci*. 2017; 108:e23003.
17. Friedmann MP, Torbeev V, Zelenay V, Sobol A, Greenwald J, Riek R. *PLoS ONE*. 2015; 10:e0143948. [PubMed: 26650386]
18. Al-Garawi ZS, McIntosh BA, Neill-Hall D, Hatimy AA, Sweet SM, Bagley MC, Serpell LC. *Nanoscale*. 2017; 9:10773–10783. [PubMed: 28722055]
19. Zhang CQ, Xue XD, Luo Q, Li YW, Yang KN, Zhuang XX, Jiang YG, Zhang JC, Liu JQ, Zou GZ, Liang XJ. *ACS Nano*. 2014; 8:11715–11723. [PubMed: 25375351]
20. Monasterio O, Nova E, Diaz-Espinoza R. *Biochem Biophys Res Commun*. 2017; 482:1194–1200. [PubMed: 27923655]
21. World Health Organization. *Public health impact of pesticides used in agriculture*. 1990.
22. Lavey BJ, Janda KD. *J Org Chem*. 1996; 61:7633–7636. [PubMed: 11667704]

23. Goldsmith M, Ashani Y, Margalit R, Nyska A, Mirelman D, Tawfik DS. *Chem Biol Interact.* 2016; 259:242–251. [PubMed: 27256520]
24. Mortland MM, Raman KV. *J Agric Food Chem.* 1967; 15:163–167.
25. Lee M, Wang T, Makhlynets OV, Wu Y, Polizzi NF, Wu H, Gosavi PM, Stöhr J, Korendovych IV, DeGrado WF, Hong M. *Proc Natl Acad Sci USA.* 2017; 114:6191–6196. [PubMed: 28566494]
26. Kirby SD, Norris JR, Smith JR, Bahnson BJ, Cerasoli DM. *Chem Biol Interact.* 2013; 203:181–185. [PubMed: 23159884]
27. Xiang DF, Kolb P, Fedorov AA, Meier MM, Fedorov LV, Nguyen TT, Sterner R, Almo SC, Shoichet BK, Raushel FM. *Biochemistry.* 2009; 48:2237–2247. [PubMed: 19159332]
28. Ugwumba IN, Ozawa K, Xu Z-Q, Ely F, Foo J-L, Herlt AJ, Coppin C, Brown S, Taylor MC, Ollis DL, Mander LN, Schenk G, Dixon NE, Otting G, Oakeshott JG, Jackson CJ. *J Am Chem Soc.* 2011; 133:326–333. [PubMed: 21162578]
29. Xu Y, Yamamoto N, Ruiz DI, Kubitz DS, Janda KD. *Bioorg Med Chem Lett.* 2005; 15:4304–4307. [PubMed: 16046128]
30. Kennedy DJ, Mayer BP, Baker SE, Valdez CA. *Inorg Chim Acta.* 2015; 436:123–131.
31. Morrow JR, Trogler WC. *Inorg Chem.* 1989; 28:2330–2333.
32. Kuo LY, Perera NM. *Inorg Chem.* 2000; 39:2103–2106. [PubMed: 12526519]
33. Filice M, Palomo JM. *ACS Catalysis.* 2014; 4:1588–1598.
34. LeBel CP, Ischiropoulos H, Bondy SG. *Chem Res Toxicol.* 1992; 5:227–231. [PubMed: 1322737]
35. Bonini MG, Rota C, Tomasi A, Mason RP. *Free Radic Biol Med.* 2006; 40:968–975. [PubMed: 16540392]

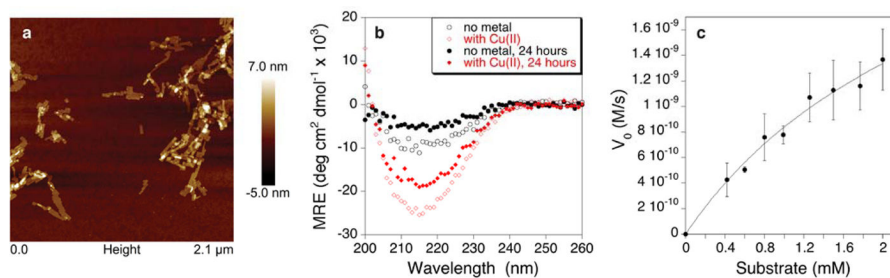


Figure 1.

7IY forms amyloid-like fibrils that catalyze paraoxon hydrolysis. a) AFM images of the fibrils formed by **7IY** in the presence of Cu^{II}; peptides were incubated for 15–30 min prior to deposition onto mica; b) CD spectra of **7IY** under various conditions ($[7IY] = [Cu^{II}] = 25 \mu M$, 5 mM HEPES, pH 8.0); c) dependence of initial rate of paraoxon hydrolysis catalyzed by **7IY** on the substrate concentration; peptides were incubated at 37 °C for 30 min prior to addition of substrate to ensure fibril formation.

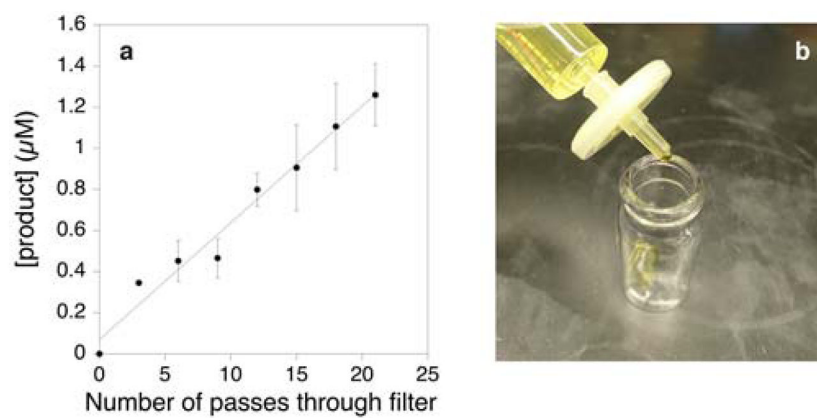
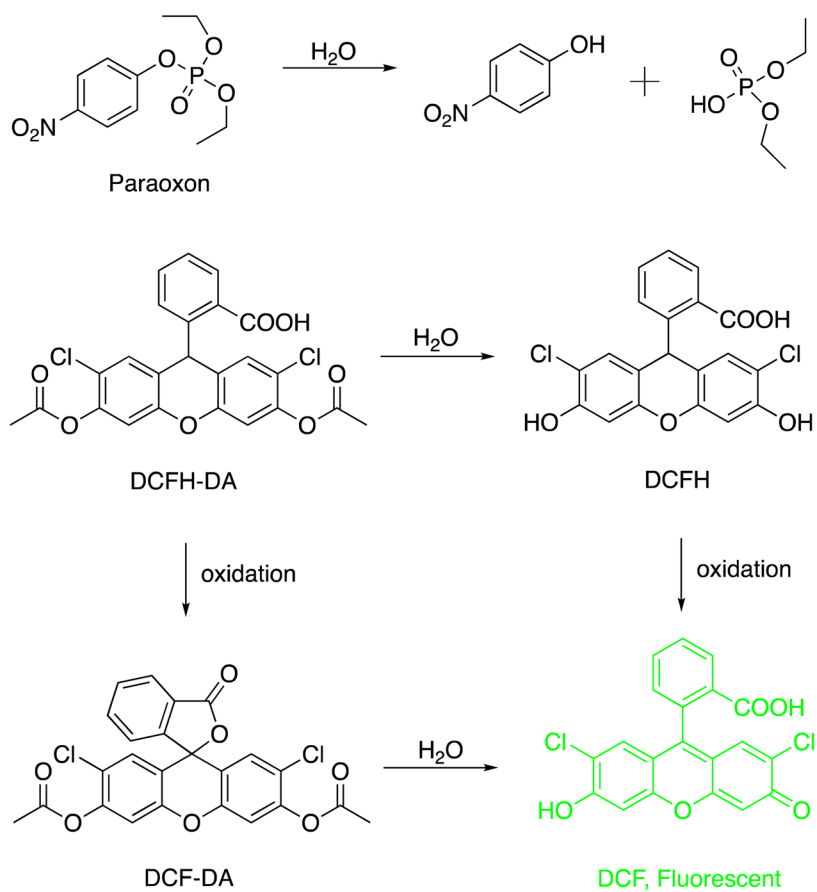


Figure 2. Hydrolysis of paraoxon facilitated by multiple passes of the substrate solution through a flow device at 1 mL/min (a) prepared by a deposition of copper-containing fibrils on PES support (b).



Scheme 1.
Hydrolysis of paraoxon and tandem reactions catalyzed by catalytic amyloids.

Table 1

Kinetic parameters for hydrolysis and/or oxidation of various fluorescein derivatives.

Substrate	Product	Catalyst	$k_2, \text{M}^{-1} \text{min}^{-1}$
DCFH-DA	DCF	7IY	61.2 ± 9.6
DCFH-DA	DCF	7IQ	97.2 ± 6.6
DCFH	DCF	7IY	288.6 ± 20.4
DCFH	DCF	7IQ	291.0 ± 23.4
DCF-DA	DCF	7IY	33.6 ± 3
DCF-DA	DCF	7IQ	30.0 ± 0.6

Author Manuscript

Author Manuscript

Author Manuscript

Author Manuscript